Energy Level Alignment of N-Doping Fullerenes and Fullerene Derivatives Using Air-Stable Dopant

Qinye Bao, Xianjie Liu, Slawomir Braun, Yanqing Li, Jianxin Tang, Chungang Duan and Mats Fahlman

Bao, Q., Liu, X., Braun, S., Li, Y., Tang, J., Duan, C., Fahlman, M., (2017), Energy Level Alignment of N-Doping Fullerenes and Fullerene Derivatives Using Air-Stable Dopant, *ACS Applied Materials and Interfaces*, 9(40), 35476-35482. https://doi.org/10.1021/acsami.7b11768

Article

Energy Level Alignment of N-Doping Fullerenes and Fullerene Derivatives Using Air-Stable Dopant

Qinye Bao,[*] Xianjie Liu, Slawomir Braun, Yanqing Li, Jianxin Tang, Chungang Duan, Mats Fahlman

Prof. Q. Bao, Prof. C. Duan
Key Laboratory of Polar Materials and Devices, Ministry of Education, East China Normal University, 200241, Shanghai, P.R. China
E-mail: qybao@clpm.ecnu.edu.cn

Dr. Q. Bao, Dr. X. Liu, Dr. S. Braun and Prof. M. Fahlman
Division of Surface Physics and Chemistry, IFM, Linköping University SE-58183 Linköping, Sweden

Prof. Y. Li, Prof. J. Tang
Institute of Functional Nano & Soft Materials (FUNSOM), Soochow University, Suzhou 215123, P. R. China

Keywords: Doping； energy level alignment； Interfaces； spectroscopy； organic semiconductor； organic electronics

Abstract

Doping has been proved to be one of the powerful technologies to achieve significant improvement in organic electronic device performance. Herein, we systematically map out the interface properties of solution processed air stable n-type 4-(1,3-dimethyl-2,3-dihydro-1H-benzoimidazol-2-yl)phenyl (DMBI) doping fullerenes and fullerene derivatives, and establish an universal energy level alignment scheme for this class of n-doped system. At low doping levels where the charge transfer doping induces mainly bound charges, the energy level alignment of the n-doping organic semiconductor can be described by combining integer charger transfer (ICT)-induced shifts with a so-called double dipole step. At high doping levels significant density of free charges are generated and charge flows between the organic film and the conducting electrodes equilibrating the Fermi level in a classic “depletion layer” scheme. Moreover, we demonstrate that the model holds for both n and p-doping of π-backbone molecules and

polymers. With the results, we provide the wide guidance for identifying application of current organic n-type doping technology in organic electronics.

Introduction

Doping of organic semiconductors have been applied in organic light-emitting diodes (OLEDs),[1-2] organic photovoltaics (OPVs),[3-5] and organic thin-film transistors (OTFTs)[6-8] to achieve significant improvement in device performance. Studies show that the doping of organic semiconductors can increase film conductivity by several orders of magnitude[9-11] and decrease the charge-injection barrier at electrodes, the latter attributed to shifts of the Fermi level,[11-14] as well as suppress the geminate charge recombination at donor-acceptor interface via filling of the so-called tail states.[15] Doping also may induce deep trap filling and hence improve the overall carrier mobility.[16] To date, several p-type doped organic systems, especially using F4TCNQ as dopant, comprehensively have been investigated and used in electronic devices.[4, 10-11, 13, 15] In contrast, knowledge and functional use of n-type doped organic system is limited. The energetics of the n-type dopant must allow electron transfer from the dopant's highest occupied molecular orbital (HOMO) to the organic semiconductor host's lowest unoccupied molecular orbital (LUMO). The n-type dopant is then typically to oxidation by oxygen/water,[17] and hence unstable in ambient atmosphere which presents a technological challenge.

Bao's group developed an air-stable molecule, (4-(1,3-dimethyl-2,3-dihydro-1H-benzoimidazol-2-yl)phenyl)(DMBI), that with its derivatives share an effective n-type doping ability.[18-20] Solution-processed DMBI doped fullerene[7], Poly(p-phenylene vinylene),[21] carbon nanotube,[22] and graphene[23] films show improved electrical

properties and higher device efficiency. A working mechanism of the DMBI doping has been outlined and involves the neutral radical formation of DMBI via hydride transfer followed by a net integer charge transfer to the host, different from simple charge transfer.[19] (The HOMO of DMBI actually lies at a higher energy, 4.1 eV Fig. S1, than the LUMO of many organic semiconductors, e.g. $PC_{60}BM$, 3.8 eV[24]).

Energy level alignment at organic/electrode and organic/organic interfaces plays a critical role in determining device performance.[25-28] The integer charge transfer (ICT) model describes the energy level alignment for the weakly-interacting interfaces obtained from physisorbed films.[29-32] Fig.1a shows the typical energy level alignment behavior at interfaces that follow the ICT model, i.e. three distinct regimes, where the resulting work function is either substrate independent (i, iii) or linearly dependent with a slope (S) of $\sim$ 1(ii). The origin of the fermi level pinning is caused by spontaneous charge transfer across the interface when the substrate work function is larger (smaller) than the energy required to oxide (gained form reducing) a molecule at the interface. The most easily oxidized/reduced molecules adjacent to the interface are used up in the process until enough charge has been transferred across the interface to create a potential step that equilibrates the Fermi level, with the resulting pinning energies being referred as the $E_{ICT+,-}$ depending on if it is positive or negative polarons created.

It was recently demonstrated that the interface for p-type doped organic system, e.g. F4TCNQ:rr-P3HT can be described by the ICT model in combination with a double step induced by image charge from $F4TCNQ^-$:rr-$P3HT^+$ charge transfer complex that cause an equivalent work function shift for the (i), (ii) and (iii) regimes.[12] In this paper, we extend that work by systematically mapping out the interface properties of solution processed n-type DMBI doping fullerene and fullerene derivatives by ultraviolet photoemission spectroscopy (UPS), and establish an energy level alignment scheme for

this class of n-doped systems. A series of C_{60}, $PC_{60}BM$ and ICBA (increasing number of adducts) act as host. The pristine host and DMBI follow the ICT model (See Fig. S2). We chose doping concentrations of 0.1%, 5% and 10% 1 w/w (dopant/host, weight ratio) to monitor the evolution of the energy level alignment from low to high doping level. To test whether organic semiconductors doped by DMBI feature similar interface properties, a host polymer poly{[N,N′-bis(2-octyldodecyl)-naphthalene-1,4,5,8-bis(dicarboximide)-2,6-diyl]-alt-5,5′-(2,2′ bithiophene)} (P(NDI2OD-T2) is studied as well. Fig. 1b shows the chemical structures of the fullerenes and P(NDI2OD-T2) employed together with the n-type dopant DMBI. The work provides experimental evidence on the general interface phenomena of air-stable DMBI doped organic semiconducting materials, which will be useful for identifying application of current organic n-type doping technology in organic electronics.

Results and Discussion

Fig. 2 displays the work function change for the DMBI-doped fullerene films on UV-ozone treated Au measured with UPS. The work function of pristine C_{60}, $PC_{60}BM$ and ICBM are 5.55, 5.26 and 5.17 eV, respectively, in agreement with previous results.[24] For C_{60}, upon doping 0.1 % DMBI, the work function reduces by 0.6 eV and reaches 4.9 eV as shown in Fig. 2a, which means that the Fermi level shifts close towards LUMO and hence decreases the electron-injection barrier, indicative of n-doping. As the doping level increases from 0.1% to 5% and 10%, the work function diminishes to 4.6 eV, where it stabilizes. Such behavior is also found for DMBI doped $PC_{60}BM$ and doped ICBA film, see Fig. 2 b and c, there is also a $\sim$ 0.6 eV work function downshift following the doping of 0.1% $PC_{60}BM$ and DMBI. The

corresponding UPS valence spectra of pristine and DMBI doped different fullerenes are depicted in Fig. 2d - f. The electronic structure features in the occupied frontier region are fully dominated by fullerenes and in shape identical to that of pristine film. The observation suggests the dopant DMBI disperse in the host matrix and does not aggregate on the surface of the films. Using the onset of HOMO peak and the work function, the ionization potential (IP) of C_{60}, $PC_{60}BM$ and ICBA are estimated to be 6.3, 6.1 and 5.9 eV, respectively. After DMBI doping, the IP does not significantly change (see Fig. S3).

Figure 3 shows the dependence of the work function of the pristine fullerene and DMBI doped fullerene films, $\Phi_{ORG/SUB}$, with doping concentrations of 0.1%, 5% and 10%, deposited onto various conducting substrates spanning a broad range of work functions, Φ_{SUB}. For the pristine C_{60}, $PC_{60}BM$ and ICBA films, two distinct slope S =0 and S =1 regions are clearly observed, following the general ICT model. In Fig 3a, when the Φ_{SUB} is larger than 5.55 eV, the Fermi level is pinned to E_{ICT+} with the formation of the downshift potential step at C_{60}/conducting substrate interface. When the Φ_{SUB} is smaller than 4.54 eV, the Fermi level is pinned to the E_{ICT-} with the formation of the upshift potential step at the interface. In the S=1 region (4.54 eV$<$ $\Phi_{SUB}<$ 5.55 eV), the $\Phi_{ORG/SUB}$ of C_{60} is equal to Φ_{SUB} *i.e.* vacuum level alignment. The E_{ICT+} (E_{ICT-}) of the pristine C_{60}, and $PC_{60}BM$ and ICBA are 5.55 (4.54), 5.26 (4.2) and 5.17 (4.07) eV, respectively, as derived from Fig 3. Upon doping 0.1% DMBI, the $\Phi_{ORG/SUB}$ of DMBI doped C_{60} in the positive Fermi level pinning region (iii) sharply shifts downward by 0.6 ~0.7 eV below the pristine film value and hence reaches 4.85 eV, but the onset of region (iii) is unaffected. The $\Phi_{ORG/SUB}$ of the negative Fermi level pinning region (i) is ~unchanged, but its corresponding threshold Φ_{SUB} extends 0.6 ~

0.7 eV, from 4.54 to 5.24 eV. In the transition region (S =1) region (ii), there is an analogous displacement of 0.6 ~0.7 eV away from Schottky-Mott limit in comparison with that of the ideal ICT model. For the high doping cases of 5% and 10%, the $\Phi_{ORG/SUB}$ of the doped C_{60} films is substrate independent over the measured range and is equal to 4.54 eV, where no S = 1 region is observed. The same interface behavior occurs for the DMBI doped $PC_{60}BM$ and ICBA systems, see Fig. 3b and c.

The findings follow our previously reported results on p-doped organic semiconductors.[33] At high doping levels where a significant densities of free charges are generated, the free charges in the organic semiconductor films flow to the substrate, creating a depletion region adjacent to the interface that equilibrates the Fermi level, which results in a substrate independent work function. Here, the 5% and 10% doped fullerenes films show a $\Phi_{ORG/SUB}$ substrate-independent behavior, in agreement with that scenario. In the case of low doping levels, the dopant-induced charge transfer does not generate free charges but rather bound electron-hole pairs.[34] Then if one of the charge species in the doped organic semiconductor film is more mobile, typically the polaron on the host as it tends to be more delocalized than the counter charge on the dopant, the more mobile (delocalized) charge can achieve a more intimate contact with the substrate. The resulting interaction with the substrate image charge is then stronger compared to the dopant-substrate image charge pair and as a consequence a double dipole step is created shifting the work function, see Fig. 4.[12, 33, 35] Here, the electrons on the n-doped fullerenes are more mobile than the localized holes left on the DMBI, resulting in two dipole moments u_1 and u_2 at the interface yielding a decreased work function, see Fig. 4, and we attribute the downshift ~ 0.6 eV from the positive pinning to S= 1 region (ii) of the 0.1 % doped fullerenes to an image charge-induced double dipole step at the interface. As observed in Fig. 3, the Φ_{SUB} for the negative pinning

region (i) has an onset-shift to higher energy by 0.6 eV compared to the ideal ICT curve of the pristine fullerenes, though the E_{ICT-} remains roughly the same. This is due to that the second and subsequent layers of DMBI:fullerene experience a new substrate consisting of the old substrate modified by the double-dipole (u_1, u_2 in Fig. 4) inducing ~monolayer. This new effective substrate will cause negative pinning of the second (and possibly subsequent) layer as long as the work function is lower than E_{ICT-} of the fullerene derivatives in the overlayer, hence the observed ~0.6 eV extension of the negative pinning region, see Fig. 3. The onset of positive pinning remains unchanged as expected, since the fullerenes in the first layer (monolayer) at the substrate does not experience the double dipole step and will be oxidized as the substrate work function exceeds the E_{ICT+}, causing pinning. The subsequent layers see an effective substrate modified both by ICT-induced dipole and the double dipole (u_1, u_2 in Fig. 4), here leading to a work function equal to the E_{ICT+} of the fullerene minus the double dipole step, as is observed. The second (and subsequent) layer thus experience an effective substrate work function substantially lower than their E_{ICT+} and hence no charge transfer will occur from these layers.

This model is expected to be general for charge-transfer-doped organic semiconductor films, so we test it on a polymer system as well: DMBI-doped P(NDI2OD-T2). P(NDI2OD-T2) has several compelling properties including high mobility and stability in air, enabling *e.g.* functionality as the acceptor material in OPVs[36-37]. Conductivity and electron spin resonance studies suggests effective n-doping through charge transfer by introducing DMBI.[38] The $\Phi_{ORG/SUB}$ of 0.1% doped polymer downshifts ~0.3 eV in comparison with the positive pinning and S= 1 region of the pristine ICT curve, as well as Φ_{SUB} onset shift to higher energy by 0. 3 eV in the negative pinning region (see Figs. S6 and S7). The doped P(NDI2OD-T2) films follow

the same trends as the doped fullerene films, suggesting that they indeed are described by the same fundamental model for the interface electronic properties. The energy shift of 0.3 eV for the DMBI doped P(NDI2OD-T2) is smaller than for the fullerenes but is in line with double dipole step values obtained for other p-doped polymers. [12] We speculate that the variation in double dipole step size between small molecules - polymers is likely originating from different charge - image charge distances, more so than differences in dielectric constant.[39]

In summary, we have studied the interface electronic properties of solution processed air stable n-type DMBI doped different fullerenes and fullerene derivatives, and established the universal energy level alignment. At low doping levels where the charge transfer doping induces mainly bound charges, the interface energetics can be described by combining ICT-induced shifts with a so-called double dipole step, [12, 33] the latter also occurring for polyelectrolyte interfaces. [35] As a result, the pristine ICT curve (Fig. 1) is modified by an additional energy shift induced by the double dipoles, that shifts the onset of negative pinning (region (i)) and shifts the resulting work function ($\Phi_{ORG/SUB}$) by the same amount. The direction of the shifts are determined by the sign of the more delocalized/mobile charge of the dopant:host system. For the DMBI:organic semiconductors in this study, the hole on DMBI was more localized causing a double dipole step of a direction charge that down-shifts $\Phi_{ORG/SUB}$ and extends the negative pinning region. At high doping levels significant density of free charges are generated and charge flows between the organic film and the substrate equilibrating the Fermi level in a classic “depletion layer” scheme. We demonstrate that the model holds for both n-doping of molecules and polymers. We believe that the

results achieved here would provide the useful guidance for identifying application of current organic n-type doping technology in organic electronics.

Experiment Section

Air stable n doping film preparation. The fullerene and fullerene derivatives including C_{60}, $PC_{60}BM$ and ICBA were used as received from Solenne BV, and the polymer P(NDI2OD-T2) from Polyera Cop. The n-type dopant DMBI was purchased from Sigma-Aldrich. The doping solutions were prepared by mixing the separate host and the DMBI molecule into o-dichlorobenzene as the desired weight ratios (dopant/host) from 0.1% to 10%. Films were spin coated on various conducting substrates with a board range of work function from 3.6 to 6.0 eV in order to create various interfaces: AlOx/Al (Φ = 3.6–3.9 eV), SiOx/Si (Φ = 4.2–4.4 eV), AuOx/Au (Φ = 4.3–4.7 eV), AgOx/Ag (Φ = 4.5–4.6 eV), ITO and UVO treatment (Φ = 4.5–4.9 eV), PEDOT:PSS (Φ = 5.0–5.2 eV), and UVO treated Au (Φ = 5.3~5.8 eV) All substrates were clean by sonication in acetone and isopropyl before spin coating.

Interface energetics characterization. Ultraviolet photoemission spectroscopy measurements were carried out in an ultrahigh vacuum (UHV) surface analysis system, consisting of an entry chamber (base pressure $\backsim$ 2 x10^{-10} mbar), a preparation chamber ($\backsim$ 8 x10^{-10} mbar) and an analysis chamber ($\backsim$ 2 x10^{-10} mbar). The spectra are recorded by Scienta-200 hemispherical analyzer. UPS was performed using HeI 21.22 eV as excitation source to detect the work function and the frontier electronic structure features. The work function is derived from the secondary electron cut-off and the ionization potential from the frontier edge of the occupied density of states with energy

resolution of 0.05 eV. All measurements were calibrated by referencing to the Fermi level of the Ar^+ ion sputter-clean gold foil.

Acknowledges: The work is sponsored by the National Science Foundation of China grant No.11604099, the Swedish Foundation for Strategic Research SE13-0060, the Swedish Research Council project grant 2016-05498, the Goran Gustafsson Foundation for Research in Nature Sciences and Medicine and the Swedish Government Strategic Research Area in Materials Science on Functional Materials at Linköping University (Faculty Grant SFO Mat LiU No 2009 00971).

Supporting Information

UPS spectra of DMBI film, ICT curve of C_{60}, $PC_{60}BM$, ICBA, P(NDI2OD-T2) and DMBI, IP distributions, work function of the increased film thickness, conductivity, UPS spectra of DMBI doped P(NDI2OD-T2) and their work function dependences on the substrate work function.

Author Information

∗Email: qybao@clpm.ecnu.edu.cn

The authors declare no competing financial interest.

References

(1). Zhou, X.; Blochwitz, J.; Pfeiffer, M.; Nollau, A.; Fritz, T.; Leo, K., Enhanced Hole Injection into Amorphous Hole-Transport Layers of Organic Light-Emitting Diodes Using Controlled P-Type Doping. *Adv. Funct. Mater.* **2001,** *11*, 310-314.

(2). Gross, M.; Muller, D. C.; Nothofer, H. G.; Scherf, U.; Neher, D.; Brauchle, C.; Meerholz, K., Improving the Performance of Doped Pi-Conjugated Polymers for Use in Organic Light-Emitting Diodes. *Nature* **2000,** *405*, 661-665.

(3). Dai, A.; Zhou, Y. H.; Shu, A. L.; Mohapatra, S. K.; Wang, H.; Fuentes-Hernandez, C.; Zhang, Y. D.; Barlow, S.; Loo, Y. L.; Marder, S. R.; Kippelen, B.; Kahn, A., Enhanced Charge-Carrier

Injection and Collection Via Lamination of Doped Polymer Layers p-Doped with a Solution-Processible Molybdenum Complex. *Adv. Funct. Mater.* **2014,** *24*, 2197-2204.
(4). Zhang, Y.; Zhou, H. Q.; Seifter, J.; Ying, L.; Mikhailovsky, A.; Heeger, A. J.; Bazan, G. C.; Nguyen, T. Q., Molecular Doping Enhances Photoconductivity in Polymer Bulk Heterojunction Solar Cells. *Adv. Mater.* **2013,** *25*, 7038-7044.
(5). Han, X. Y.; Wu, Z. W.; Sun, B. Q., Enhanced Performance of Inverted Organic Solar Cell by a Solution-Based Fluorinated Acceptor Doped P3HT:PCBM Layer. *Org. Electron.* **2013,** *14*, 1116-1121.
(6). Abe, Y.; Hasegawa, T.; Takahashi, Y.; Yamada, T.; Tokura, Y., Control of Threshold Voltage in Pentacene Thin-Film Transistors using Carrier Doping at the Charge-Transfer Interface with Organic Acceptors. *Appl. Phys. Lett.* **2005,** *87*, 153506.
(7). Rossbauer, S.; Muller, C.; Anthopoulos, T. D., Comparative Study of the N-Type Doping Efficiency in Solution-processed Fullerenes and Fullerene Derivatives. *Adv. Funct. Mater.* **2014,** *24*, 7116-7124.
(8). Wei, P.; Oh, J. H.; Dong, G. F.; Bao, Z. N., Use of a 1H-Benzoimidazole Derivative as an n-Type Dopant and To Enable Air-Stable Solution-Processed n-Channel Organic Thin-Film Transistors. *J. Am. Chem. Soc.* **2010,** *132*, 8852-8853.
(9). Yim, K. H.; Whiting, G. L.; Murphy, C. E.; Halls, J. J. M.; Burroughes, J. H.; Friend, R. H.; Kim, J. S., Controlling Electrical Properties of Conjugated Polymers via a Solution-based P-Type Doping. *Adv. Mater.* **2008,** *20*, 3319-3324.
(10). Duong, D. T.; Wang, C. C.; Antono, E.; Toney, M. F.; Salleo, A., The Chemical and Structural Origin of Efficient P-Type Doping in P3HT. *Org. Electron.* **2013,** *14*, 1330-1336.
(11). Pingel, P.; Neher, D., Comprehensive Picture of P-Type Doping of P3HT with the Molecular Acceptor F4TCNQ. *Phy. Rev. B* **2013,** *87*, 115209.
(12). Bao, Q. Y.; Liu, X. J.; Braun, S.; Gao, F.; Fahlman, M., Energetics at Doped Conjugated Polymer/Electrode Interfaces. *Adv. Mater. Interfaces* **2015,** *2*, 1400403.
(13). Gao, W. Y.; Kahn, A., Controlled P Doping of the Hole-Transport Molecular Material N,N '-diphenyl-N,N '-bis(1-naphthyl)-1,1(')-biphenyl-4,4 '-diamine with Tetrafluorotetracyanoquinodimethane. *J. Appl. Phys.* **2003,** *94*, 359-366.
(14). Bin, Z. Y.; Li, J. W.; Wang, L. D.; Duan, L., Efficient N-type Dopants with Extremely Low Doping Ratios for High Performance Inverted Perovskite Solar Cells. *Energy Environ. Sci.* **2016,** *9*, 3424-3428.
(15). Deschler, F.; Da Como, E.; Limmer, T.; Tautz, R.; Godde, T.; Bayer, M.; von Hauff, E.; Yilmaz, S.; Allard, S.; Scherf, U.; Feldmann, J., Reduced Charge Transfer Exciton Recombination in Organic Semiconductor Heterojunctions by Molecular Doping. *Phys. Rev. Lett.* **2011,** *107*, 127402.
(16). Ma, L.; Lee, W. H.; Park, Y. D.; Kim, J. S.; Lee, H. S.; Choa, K., High Performance Polythiophene Thin-Film Transistors Doped with Very Small Amounts of an Electron Acceptor. *Appl. Phys. Lett.* **2008,** *92*, 063310.
(17). Walzer, K.; Maennig, B.; Pfeiffer, M.; Leo, K., Highly Efficient Organic Devices Based on Electrically Doped Transport Layers. *Chem. Rev.* **2007,** *107*, 1233-1271.
(18). Wei, P.; Menke, T.; Naab, B. D.; Leo, K.; Riede, M.; Bao, Z., 2-(2-Methoxyphenyl)-1,3-dimethyl-1H-benzoimidazol-3-ium Iodide as a New Air-Stable n-Type Dopant for Vacuum-Processed Organic Semiconductor Thin Films. *J. Am. Chem. Soc.* **2012,** *134*, 3999-4002.
(19). Naab, B. D.; Guo, S.; Olthof, S.; Evans, E. G. B.; Wei, P.; Millhauser, G. L.; Kahn, A.; Barlow, S.; Marder, S. R.; Bao, Z. A., Mechanistic Study on the Solution-Phase n-Doping of 1,3-Dimethyl-2-aryl-2,3-dihydro-1H-benzoimidazole Derivatives. *J. Am. Chem. Soc.* **2013,** *135*, 15018-15025.
(20). Naab, B. D.; Himmelberger, S.; Diao, Y.; Vandewal, K.; Wei, P.; Lussem, B.; Salleo, A.; Bao, Z. N., High Mobility N-Type Transistors Based on Solution-Sheared Doped 6,13-Bis(triisopropylsilylethynyl)pentacene Thin Films. *Adv. Mater.* **2013,** *25*, 4663-4667.

(21). Lu, M. T.; Nicolai, H. T.; Wetzelaer, G. J. A. H.; Blom, P. W. M., N-Type Doping of Poly(p-phenylene vinylene) with Air-Stable Dopants. *Appl. Phys. Lett.* **2011,** *99*, 173302.
(22). Wang, H. L.; Wei, P.; Li, Y. X.; Han, J.; Lee, H. R.; Naab, B. D.; Liu, N.; Wang, C. G.; Adijanto, E.; Tee, B. C. K.; Morishita, S.; Li, Q. C.; Gao, Y. L.; Cui, Y.; Bao, Z. N., Tuning the Threshold Voltage of Carbon Nanotube Transistors by N-Type Molecular Doping for Robust and Flexible Complementary Circuits. *PNAS* **2014,** *111*, 4776-4781.
(23). Wei, P.; Liu, N.; Lee, H. R.; Adijanto, E.; Ci, L. J.; Naab, B. D.; Zhong, J. Q.; Park, J.; Chen, W.; Cui, Y.; Bao, Z. A., Tuning the Dirac Point in CVD-Grown Graphene through Solution Processed n-Type Doping with 2-(2-Methoxyphenyl)-1,3-dimethyl-2,3-dihydro-1H-benzoimidazole. *Nano. Lett.* **2013,** *13*, 1890-1897.
(24). Bao, Q. Y.; Sandberg, O.; Dagnelund, D.; Sanden, S.; Braun, S.; Aarnio, H.; Liu, X. J.; Chen, W. M. M.; Osterbacka, R.; Fahlman, M., Trap-Assisted Recombination via Integer Charge Transfer States in Organic Bulk Heterojunction Photovoltaics. *Adv. Funct. Mater.* **2014,** *24*, 6309-6316.
(25). Ma, H.; Yip, H. L.; Huang, F.; Jen, A. K. Y., Interface Engineering for Organic Electronics. *Adv. Funct. Mater.* **2010,** *20*, 1371-1388.
(26). Chen, L. M.; Xu, Z.; Hong, Z. R.; Yang, Y., Interface Investigation and Engineering - Achieving High Performance Polymer Photovoltaic Devices. *J. Mater. Chem.* **2010,** *20*, 2575-2598.
(27). Ishii, H.; Sugiyama, K.; Ito, E.; Seki, K., Energy Level Alignment and Interfacial Electronic Structures at Organic/Metal and Organic/Organic Interfaces *Adv. Mater.* **1999,** *11*, 972-972.
(28). Bao, Q. Y.; Yang, J. P.; Xiao, Y.; Deng, Y. H.; Lee, S. T.; Li, Y. Q.; Tang, J. X., Correlation between the Electronic Structures of Transition Metal Oxide-Based Intermediate Connectors and the Device Performance of Tandem Organic Light-Emitting Devices. *J. Mater. Chem.* **2011,** *21*, 17476-17482.
(29). Braun, S.; Salaneck, W. R.; Fahlman, M., Energy-Level Alignment at Organic/Metal and Organic/Organic Interfaces. *Adv. Mater.* **2009,** *21*, 1450-1472.
(30). Sehati, P.; Braun, S.; Lindell, L.; Liu, X. J.; Andersson, L. M.; Fahlman, M., Energy-Level Alignment at Metal-Organic and Organic-Organic Interfaces in Bulk-Heterojunction Solar Cells. *IEEE J. Sel. Top Quant.* **2010,** *16*, 1718-1724.
(31). Fahlman, M.; Crispin, A.; Crispin, X.; Henze, S. K. M.; de Jong, M. P.; Osikowicz, W.; Tengstedt, C.; Salaneck, W. R., Electronic Structure of Hybrid Interfaces for Polymer-Based Electronics. *J. Phys. Condens. Mat.* **2007,** *19*, 183202.
(32). Greiner, M. T.; Helander, M. G.; Tang, W. M.; Wang, Z. B.; Qiu, J.; Lu, Z. H., Universal Energy-Level Alignment of Molecules on Metal Oxides. *Nat. Mater.* **2012,** *11*, 76-81.
(33). Bao, Q.; Liu, X.; Wang, E.; Fang, J.; Gao, F.; Braun, S.; Fahlman, M., Regular Energetics at Conjugated Electrolyte/Electrode Modifier for Organic Electronics and their Implications on Design Rules. *Adv. Mater. Interfaces* **2015,** *2*, 1500204.
(34). Mityashin, A.; Olivier, Y.; Van Regemorter, T.; Rolin, C.; Verlaak, S.; Martinelli, N. G.; Beljonne, D.; Cornil, J.; Genoe, J.; Heremans, P., Unraveling the Mechanism of Molecular Doping in Organic Semiconductors. *Adv. Mater.* **2012,** *24*, 1535-1539.
(35). van Reenen, S.; Kouijzer, S.; Janssen, R. A. J.; Wienk, M. M.; Kemerink, M., Origin of Work Function Modification by Ionic and Amine-Based Interface Layers. *Adv. Mater. Interfaces* **2014,** *1*, 1400189.
(36). Li, Z.; Lin, J. D. A.; Phan, H.; Sharenko, A.; Proctor, C. M.; Zalar, P.; Chen, Z. H.; Facchetti, A.; Nguyen, T. Q., Competitive Absorption and Inefficient Exciton Harvesting: Lessons Learned from Bulk Heterojunction Organic Photovoltaics Utilizing the Polymer Acceptor P(NDI2OD-T2). *Adv. Funct. Mater.* **2014,** *24*, 6989-6998.
(37). Tang, Y. Q.; McNeill, C. R., All-Polymer Solar Cells Utilizing Low Band Gap Polymers as Donor and Acceptor. *J. Polym. Sci. Pol. Phys.* **2013,** *51*, 403-409.

(38). Schlitz, R. A.; Brunetti, F. G.; Glaudell, A. M.; Miller, P. L.; Brady, M. A.; Takacs, C. J.; Hawker, C. J.; Chabinyc, M. L., Solubility-Limited Extrinsic n-Type Doping of a High Electron Mobility Polymer for Thermoelectric Applications. *Adv. Mater.* **2014,** *26*, 2825-2830.
(39). Liu, F.; Page, Z. A.; Duzhko, V. V.; Russell, T. P.; Emrick, T., Conjugated Polymeric Zwitterions as Efficient Interlayers in Organic Solar Cells. *Adv. Mater.* **2013,** *25*, 6868-6873.

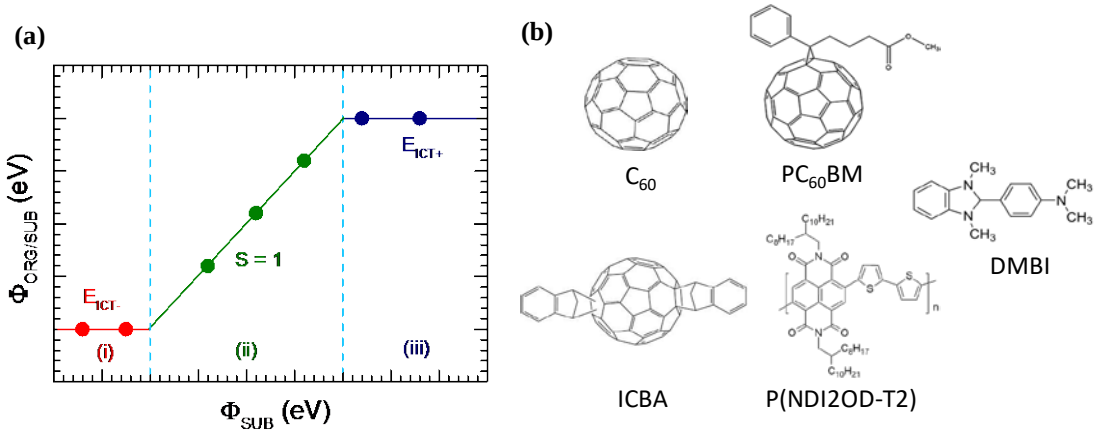

Figure 1. (a) Typical energy level alignment regimes for organic semiconductor weakly interacting interfaces according to the ICT model, where the resulting work function, $\Phi_{ORG/SUB}$, is either substrate independent (i, iii) or linearly dependent with a slope of (S) =1. (b) Chemical structures of the host fullerenes, polymer P(NDI2OD-T2) and the n-type dopant DMBI molecule in this study.

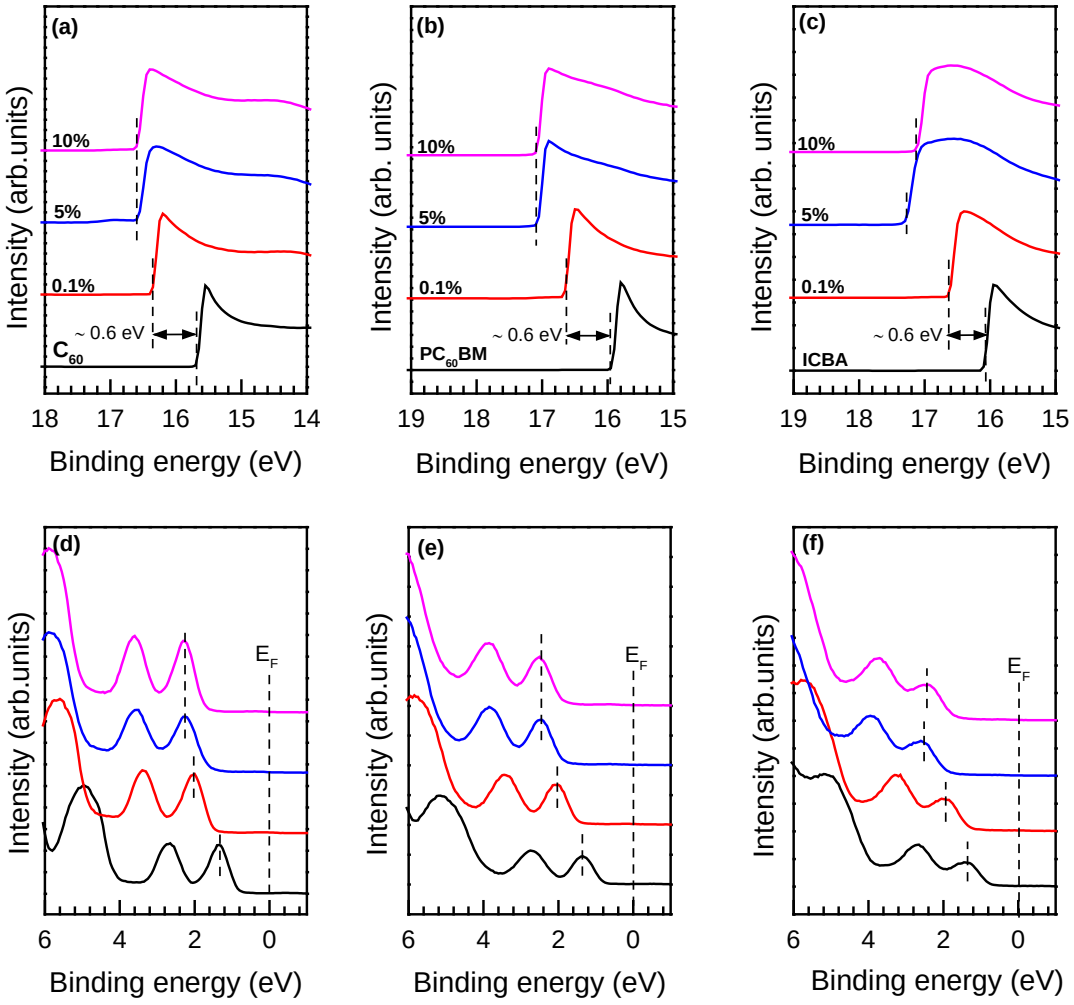

Figure 2. UPS spectra evolutions at the secondary electron region (work function) and the frontier electronic structure region (HOMO) of n-type DMBI doped C_{60} (a, d), $PC_{60}BM$ (b, e) and ICBA(c, f) film with doping concentrations of 0.1%, 5% and 10% on UV-ozone treated Au.

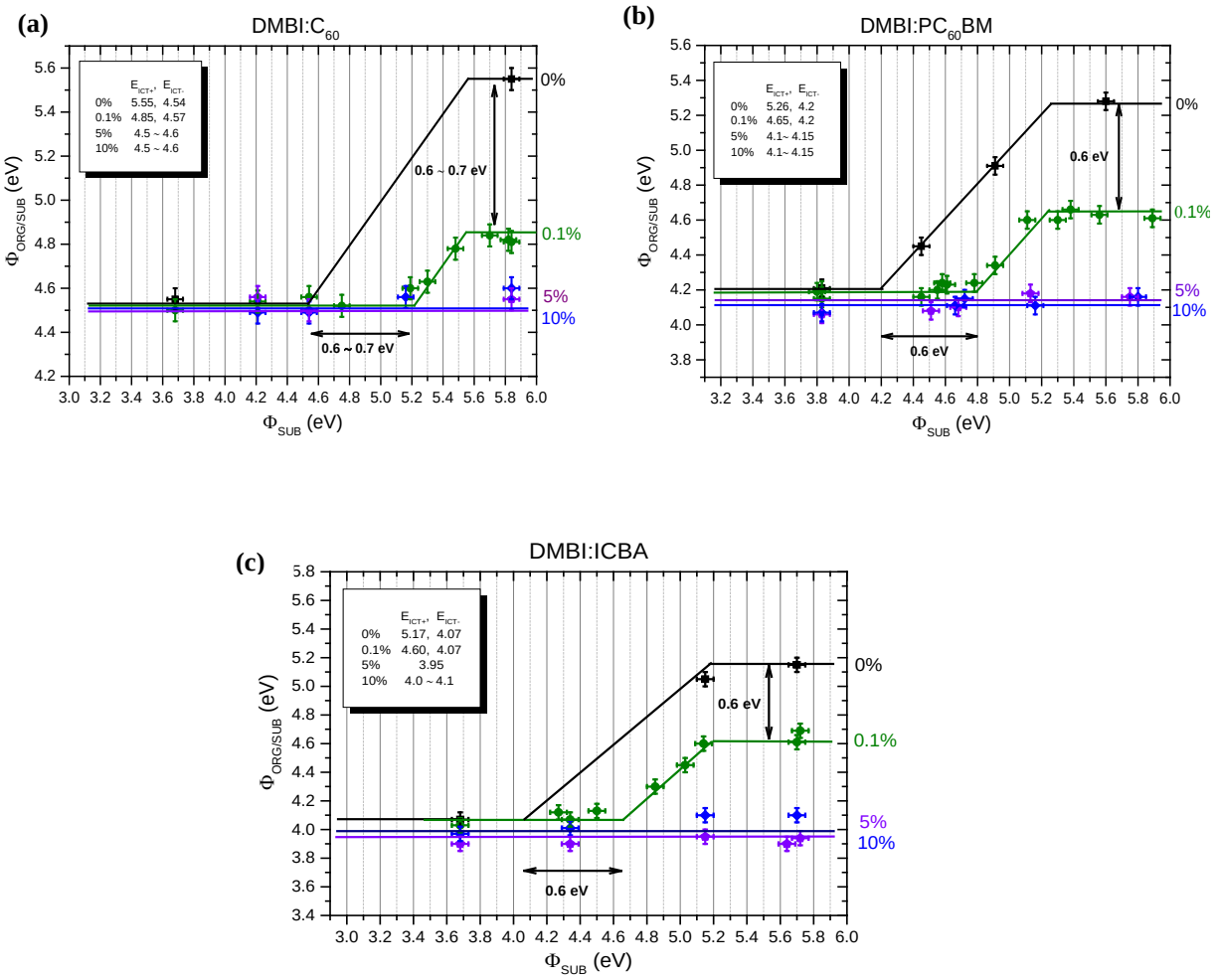

Figure 3. Dependences of the work function of the pristine fullerenes and DMBI doped (a) C_{60}, (b) $PC_{60}BM$, (c) ICBA films with doping concentrations of 0.1%, 5% and 10%, $\Phi_{ORG/SUB}$, deposited onto various conducting substrates spanning a broad range of work functions, Φ_{SUB}. The energy error in measurement is ± 0.05 eV.

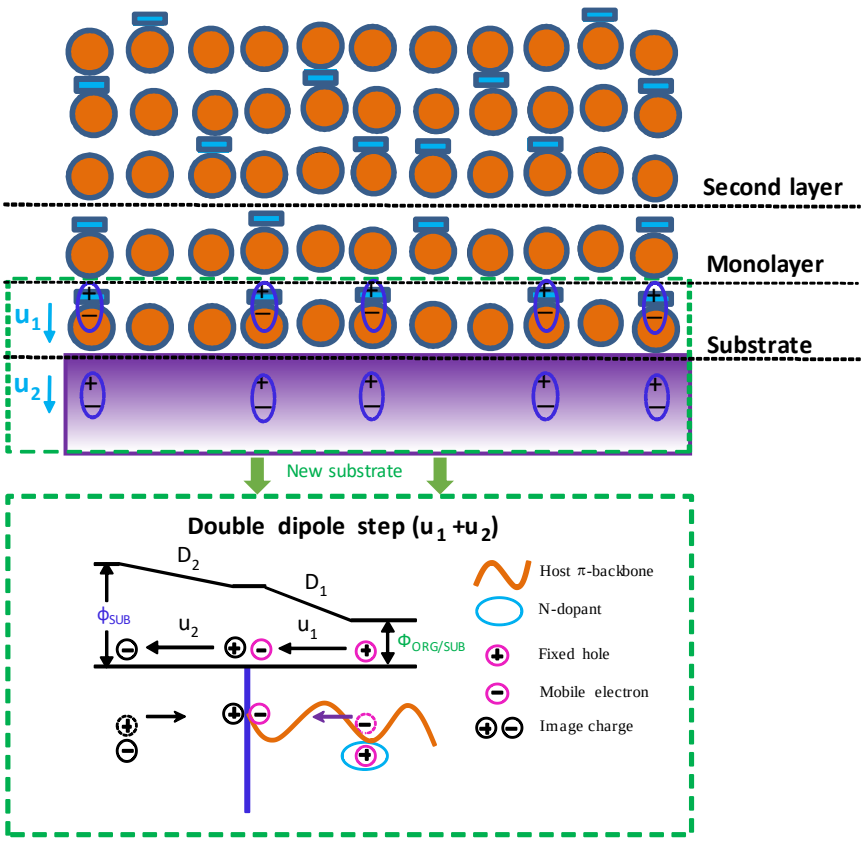

Figure 4. General model for energy level alignment of molecular n-doped organic semiconductors at low doping concentration. Relative to the fixed holes of the n-type dopant molecule (here DMBI), the electrons on the host π –backbone (here fullerene derivatives and P(NDI2OD-T2)) are more mobile than the holes. (Note dopant density highly exaggerated). This process produces the two dipole moments u_1 and u_2 at the interface, yielding a decrease in work function of the doped film (D_1 + D_2). An additional potential shift may occur through integer charge transfer across an interface as per the ICT model, yielding the Fermi level pinning effect in region (i) and (iii). Note that the molecules/polymers in the first layer (monolayer) at the substrate does not experience the double dipole step, whereas subsequent layers experience a substrate work function modified by it.

Table of Contents:

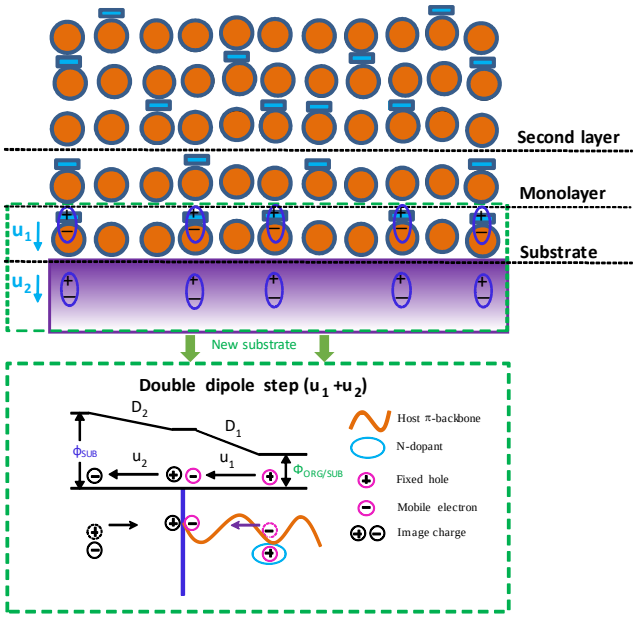

Supporting Information

Energy Level Alignment of N-Doping Fullerenes and Fullerene Derivatives Using Air-Stable Dopant

Qinye Bao, Xianjie Liu, Slawomir Braun, Yanqing Li, Jianxin Tang, Chungang Duan, Mats Fahlman*

Prof. Q. Bao, Prof. C. Duan
Key Laboratory of Polar Materials and Devices, Ministry of Education, East China Normal University, 200241, Shanghai, P.R. China
E-mail: qybao@clpm.ecnu.edu.cn

Dr. Q. Bao, Dr. X. Liu, Dr. S. Braun and Prof. M. Fahlman
Division of Surface Physics and Chemistry, IFM, Linköping University SE-58183 Linköping, Sweden

Prof. Y. Li, Prof. J. Tang
Institute of Functional Nano & Soft Materials (FUNSOM), Soochow University, Suzhou 215123, P. R. China

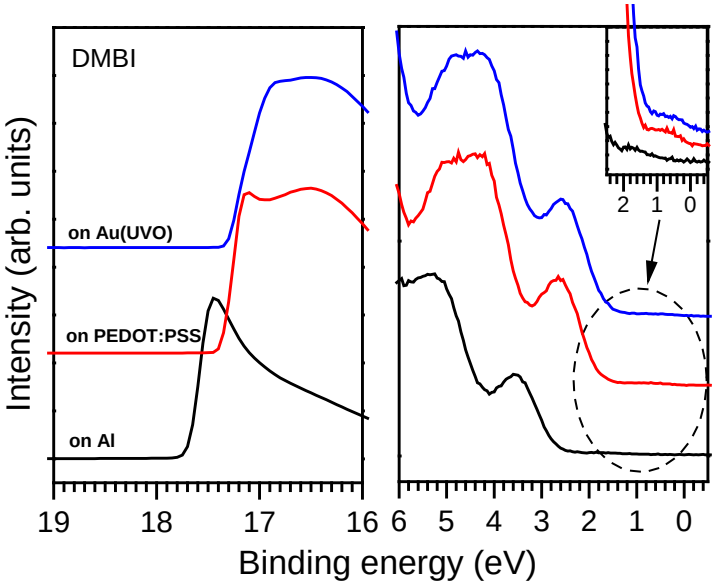

Figure S1. UPS spectra for DMBI film coated on Al, PEDOT:PSS and Au(UVO), respectively. The work function in combination with the onset of HOMO peak, the ionization potential/ HOMO of DMBI film is 4.1 eV.

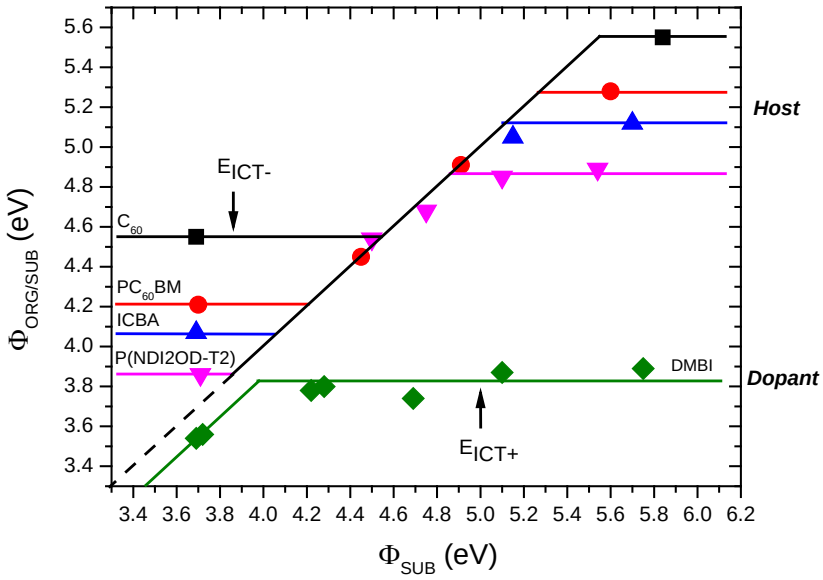

Figure S2. The ICT curves of the host organic semiconductors C_{60}, $PC_{60}BM$, ICBA, P(NDI2OD-T2) and the dopant molecule DMBI. The energy shift of DMBI in S =1 region results from the mobile proton-induced dipole at interface.

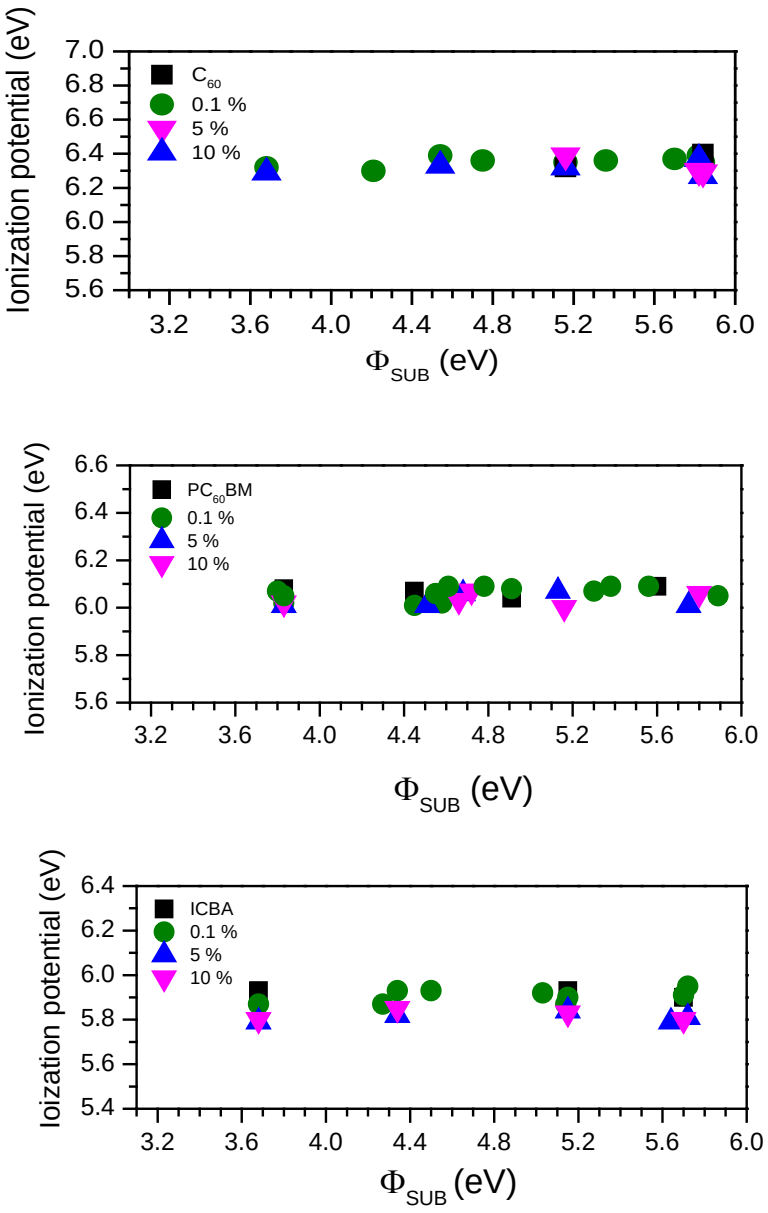

Figure S3. Vertical ionization potential of the pristine and DMBI doped C_{60}, $PC_{60}BM$ and ICBA films on various substrates.

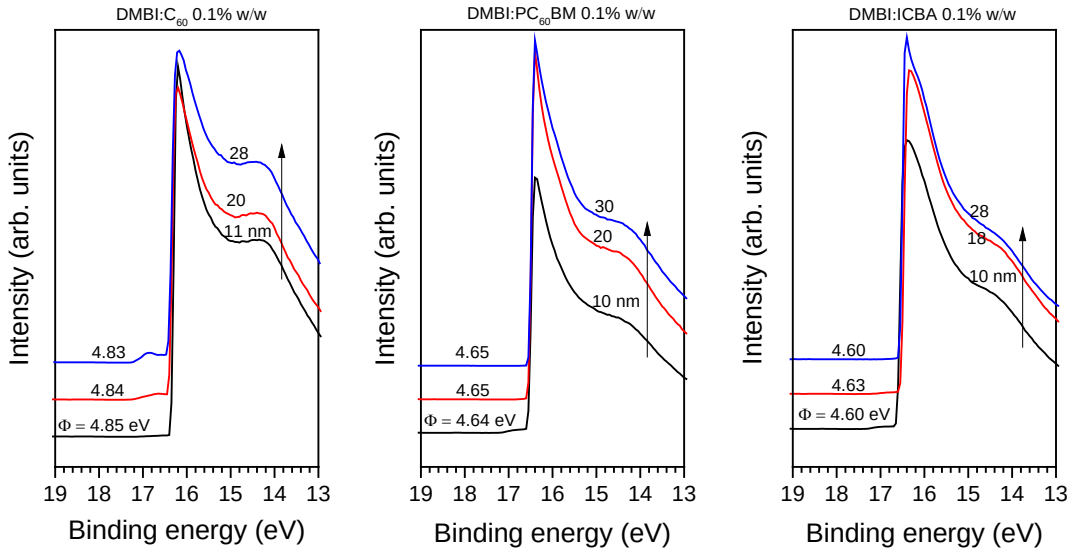

Figure S4. UPS spectra in work function region for DMBI doped C_{60}, $PC_{60}BM$ and ICBA (0.1% w/w) with different thickness on UV-ozone treated Au.

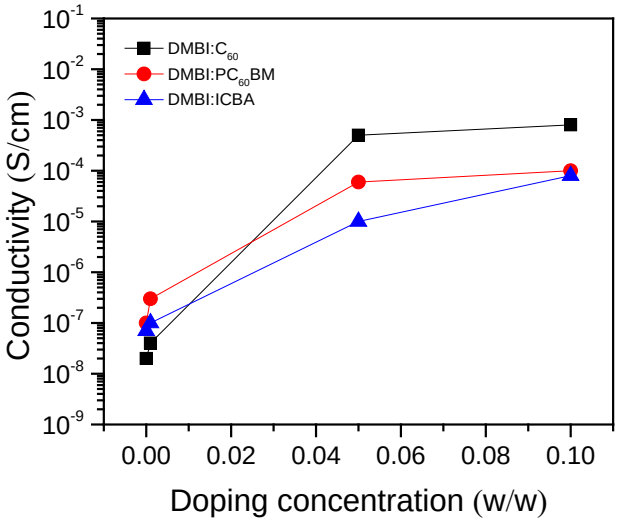

Figure S5. Electrical conductivity of DMBI doped C_{60}, $PC_{60}BM$ and ICBA film with doping concentrations of 0.1%, 5% and 10% w/w.

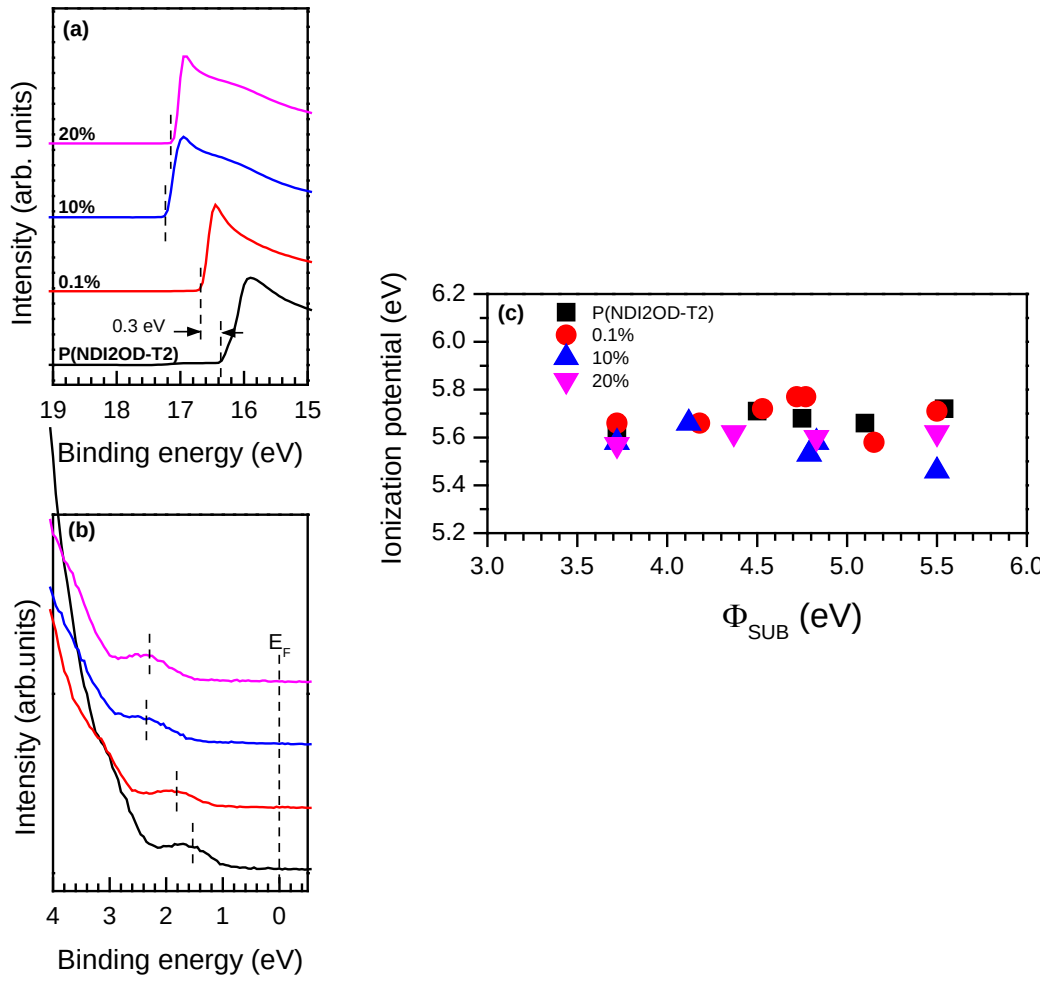

Figure S6. UPS spectra evolutions at (a) the secondary electron region (work function) and (b) the frontier electronic structure region (HOMO) of n-type DMBI doped P(NDI2OD-2) film on substrate Au(UVO); (c) Vertical ionization potential of the pristine and DMBI doped P(NDI2OD-2) films with doping concentrations of 0.1%, 10% and 20%, on various substrates.

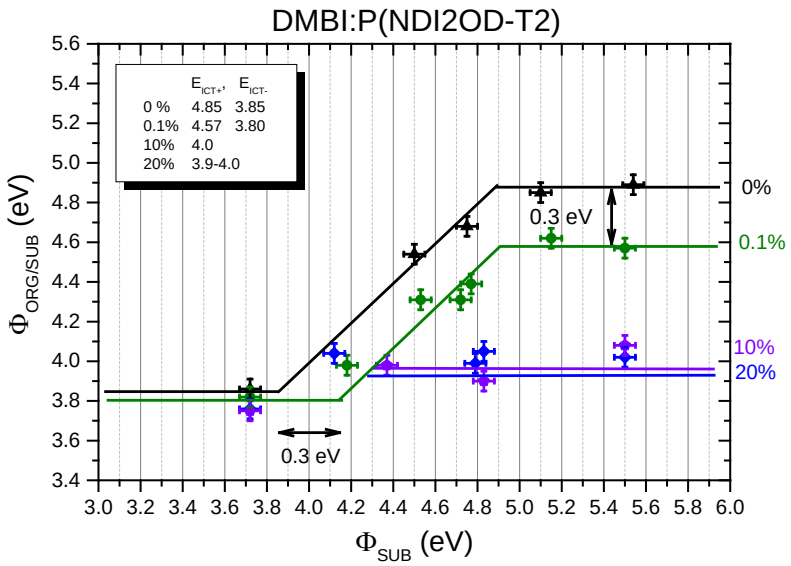

Figure S7. Dependences of the work function of the DMBI doped polymer P(NDI2OD-T2) with doping concentrations of 0.1%, 10% and 20% on the work function of the various substrates.